

Preparation and characterization of ZSM5-supported nano-zero-valent iron and its potential application in nitrate remediation from aqueous solution

M. Shekarriz¹ · Z. Ramezani² · F. Elhami³

Received: 28 May 2016/Revised: 29 September 2016/Accepted: 20 December 2016/Published online: 2 January 2017
© Islamic Azad University (IAU) 2017

Abstract Zeolite Socony Mobil-5 (ZSM5)-supported nano-zero-valent iron (NZVI@ZSM5) was synthesized using homogenous precipitation method. The prepared particles were characterized by transmission electron microscope (TEM), field emission scanning electron microscope (FESEM), atomic force microscope, X-ray diffraction spectroscopy and Brunauer–Emmett–Teller as well as Fourier transform spectroscopy. The TEM image confirms the formation of NZVI particles with average size of 15 nm within ZSM5 pores. Moreover, the ability of the NZVI@ZSM5 in nitrate removal from industrial wastewaters was tested. The effects of different parameters such as solution pH, NZVI@ZSM5-nitrate solution contact time, amounts of NZVI@ZSM5, initial nitrate concentration and nitrate solution volume on removal efficiency were investigated. More than 97% nitrate ion was removed at pH = 2.5, 30 min contact time, and 0.55 g NZVI@ZSM5 for 100 mL of 50 µg mL⁻¹ nitrate. It was also shown that among the four fitted adsorption isotherms, Langmuir isotherm gives the best description of the adsorption process.

Kinetic studies showed that nitrate removal using NZVI@ZSM5 obeys pseudo-second-order kinetics ($R^2 = 0.9998$). The present method was successfully applied to the removal of nitrate contents of different wastewater gathered from the different industries located in the Khuzestan province, Iran. The reduction in their nitrate contents was in the range of 94–99%.

Keywords Nitrate removal · ZSM5 · NZVI@ZSM5 · Industrial wastewater · Zero-valent iron

Introduction

Nitrate removal from drinking and waste water is of vital importance since the toxicity and especially carcinogenicity of the high level of nitrate on both human and animals is reported. Therefore, a vast varieties of nitrate remediation procedures have been introduced. Some researchers reported chemical reduction methods. In these methods, nitrate is converted to nitrite, ammonium ion or nitrogen gas (James 2000; Gómez et al. 2002; Wang et al. 2009; Li et al. 2010; Devadas et al. 2011; Kassaei et al. 2011; Pan et al. 2012). Denitrification using different living organisms is another method for nitrate remediation from aqueous media (Rajakumar et al. 2008; Ayyasamy et al. 2009; Zhang et al. 2009; Ma et al. 2010; Zhao et al. 2011). Water desalination by reverse osmosis and membrane filtrations remove nitrate as well (Baek and Yang 2004; Tepuš et al. 2009; Kumar and Goel 2010). There are a vast variety of methods which take advantage of nitrate adsorption on the surface of a suitable sorbent (Öztürk and Bektas 2004; Yuh-Shan 2005; Cengeloglu et al. 2006; Mena-Duran et al. 2007; Wang et al. 2007a, b; Chatterjee et al. 2009; Chatterjee and Woo 2009; Demiral and

Editorial responsibility: Binbin Huang.

Electronic supplementary material The online version of this article (doi:10.1007/s13762-016-1213-y) contains supplementary material, which is available to authorized users.

✉ Z. Ramezani
zramezani@ajums.ac.ir

¹ Research Institute of Petroleum Industry (RIPI), West Blvd., Near Azadi Sports Complex, Tehran, Iran

² Nano-Technology Research Center, Ahvaz Jundishapur University of Medical Sciences, Ahvaz, Iran

³ Department of Applied Chemistry, Faculty of Chemistry, Shiraz Payame-Noor University, Shiraz, Iran

Gündüzoglu 2009; Tepuš et al. 2009; Bhatnagar et al. 2010; Cho et al. 2011; Islam and Patel 2011; Katal et al. 2011; Zhan et al. 2011; Bhardwaj et al. 2012; Xu et al. 2012). The objectives of all developed methods are to introduce simple, rapid, low cost, and environmentally green as well as high-efficient removal process.

Zero-valent iron removes nitrate through oxidation–reduction reaction (Westerhoff and James 2003). But it takes a long time due to the low reduction rate. NZVI shows more efficient and rapid nitrate remediation. These changes in the behavior of macro- and nano-iron are mainly because of the differences in their specific surface area (Kassaei et al. 2011; Pan et al. 2012; Karimi et al. 2014; Liu et al. 2014; Su et al. 2014; Wang et al. 2014). The main problems of NZVI are high reactivity and aggregation. It reacts rapidly with atmospheric oxygen as exposed to the air, then making its handling and weighing difficult. To solve these problems, two methods, namely surface coating using different materials such as surfactants (Shekarriz et al. 2010) and using different supports for the particles, are suggested by researchers. When surfactants are used, they release into aqueous media and increase TOC. Therefore, researchers prefer to use different support such as resin (Park et al. 2009), bentonite (Shi et al. 2011), kaolinite (Chen et al. 2013) and pillared clay (Zhang et al. 2011) as well as carbon (Busch et al. 2015) to maintain the synthesized nanoparticles. NZVI usually penetrates into the pore of the support and has shown more stability, decreased aggregation and low reaction with atmosphere, compared to the uncoated one (Zhang et al. 2011).

ZSM5 is a highly porous zeolite contains different metal oxides. The very regular 3-D structure and the acidity of ZSM5 can be utilized for acid-catalyzed reactions such as hydrocarbon isomerization and the alkylation of hydrocarbons (Dyer 1988; Bjørgen et al. 2008); sometimes, ZSM5 is modified with other metals or metal oxide to increase the catalytic activity. These particles cannot adsorb pollutants strongly. However, surface modification increases their sorption capacity (Zhan et al. 2011).

The aim of this study is to prepare new supported NZVI with the purpose of increasing its availability and stability in the environmental remediation. Furthermore, its application in the nitrate remediation of aqueous wastes is investigated. In the end, the results are compared with the other similar reported methods of nitrate removal from aqueous solutions.

Materials and methods

Materials and Instrument

All chemical used in this study such as potassium nitrate, hydrochloric and nitric acid, and potassium hydroxide was purchased from Merck (Darmadshdat, Germany) and used

without further purification. ZSM5 was prepared from Zeolyst international company (USA) with the following specification: $\text{SiO}_2/\text{Al}_2\text{O}_3 = 30$, $\text{Na}_2\text{O} = 0.05\%$ and surface area $405 \text{ m}^2/\text{g}$ (sample CBV 3024E).

X-ray diffraction (XRD) analyses were performed using a Philips X-ray diffractometer PW1840 with $\text{Cu}\alpha$ radiation ($\gamma = 0.154 \text{ nm}$). Representative transmission electron microscope (TEM) images of nanoparticles were obtained using a Philips CM 120 electron microscope (Netherlands). Field emission scanning electron microscopy (FESEM) and energy-dispersive spectroscopy (EDS) were used via a Mira 3-XMU microscope (Czech Republic). Samples were coated with gold before investigations. NanoWizard II, JPK (Germany) was used to record AFM images. BET surface area was determined by N_2 physisorption using a Micromeritics ASAP 3020 automated (USA). FTIR spectrum was recorded by Vertex70, Bruker (Germany). CTA 3000 Anal Tech (England) atomic absorption spectrometer was used to calculate the iron contents of NZVI@ZSM5. Metrohm pH meter was used for all pH adjustments. Nitrate concentrations were determined by ASTM standard method using Lambda45 PerkinElmer UV/Vis spectrophotometer (England). VS-8480 shaking incubator (Korea) was used for agitating purposes.

Iron content of NZVI@ZSM5 after dissolution in nitric acid was determined by flame atomic absorption spectroscopy. The iron content was determined to be 23.5%.

Preparation of NZVI@ZSM5

A solution of iron (III) chloride was prepared by dissolving 6 g anhydrous FeCl_3 (0.036 mol) in a solvent mixture consists of 100 mL EtOH and 30 mL deionized water. Two grams of the zeolite (ZSM5) was added to the clear solution of FeCl_3 (0.036 mol). Then, a solution which was prepared by dissolving 4.5 g of potassium borohydride (0.08 mol) in 20 ml of deionized water was gradually added and completely mixed with the above-prepared mixture of ZSM5 and FeCl_3 under constant vigorous stirring. Stirring was continued for 1 h after the formation of a black mixture. Then, the products were separated and washed several times with water, absolute ethanol and acetone, respectively. All reactions were run under nitrogen atmosphere. All of the solutions and solvents were purged with N_2 before use.

Remediation procedure

Stock solution: potassium nitrate was dried for about 24 h in an oven at 105°C . Accurate amount of 0.7218 g potassium nitrate was dissolved in distilled water and diluted to 1 L. The resulting solution is $100 \mu\text{g mL}^{-1}$

N-NO₃. Working solutions were prepared from this solution by successive dilution.

pH of 100 mL of the sample or standard solutions was adjusted using 0.1M HCl and 0.1M NaOH solution. Then, 0.55 g NZVI@ZSM5 was added, and the resulting mixture was agitated at 350 rpm for about 30 min. The particles were removed from the solution using 1.4T magnet. Nitrate concentrations before and after the particles contact were determined by the spectrophotometer at two wavelengths $\lambda = 220$ and 275 nm according to procedure described in the standard method for water and wastewater analysis. Percent nitrate removed was determined by Eq. (1) in which C_i is the initial nitrate concentration and C_e is the equilibrium nitrate concentration after removal.

$$\% \text{Removed} = \frac{C_i - C_e}{C_i} \times 100 \quad (1)$$

Results and discussion

NZVI@ZSM5 characterization

The synthesized particles were characterized by XRD, TEM, FTIR and FAAS as well as BET.

Figure 1c shows the X-ray diffraction patterns of NZVI@ZSM5. The iron nanoparticles of this study are rather amorphous, but a weak peak around 2 θ –44° that is the main peak of iron is identified. Other peaks are related to metal oxides in ZSM5. The color changes in ZSM5 on NZVI loading from white to black is the first visual indication of NZVI@ZSM5 preparation.

ZSM5 and NZVI@ZSM5 were separately dispersed in ethanol by ultrasonic agitation. Then, one drop of the resulting suspensions was spread over mica sheet and allowed to dry. Finally, their AFM image was recorded. Three dimension AFM images of ZSM5 and NZVI@ZSM5 are shown in Fig. 1. The average diameter of ZSM5 particles is 354.1 nm and that of NZVI@ZSM5 is 48.17 nm. Figure 1 also demonstrates that although ZSM5 aggregates extensively in the solution, NZVI@ZSM5 is more dispersed.

The TEM image of NZVI@ZSM5 is shown in Fig. 1d. It shows the formation of NZVI inside the ZSM5 pores. The image also identifies that NZVIs are amorphous and have an average size of 15 nm. The particle size of NZVI@ZSM5 observed in TEM image is smaller than that of AFM. It may be due to the aggregations of the magnetic nanoparticles while AFM cantilever moves along the surface.

Figure 2a displays the FESEM images of synthesized NZVI@ZSM5. FESEM shows that the average particle size is 10 nm. It is consistent with TEM results that show average diameters of 15 nm. Produced particles have rather spherical shapes. EDXS spectrum of resulting

nanoparticles that is shown in Fig. 2b identified iron along with the zeolite constituents (Al and Si oxides).

BET surface area of NZVI@ZSM5 was obtained by N₂ physisorption. It was 80 m²g⁻¹. This decrease in the surface area compared to ZSM5 (405 m²/g) may be attributed to the formation of NZVI in ZSM5 pores. Although the specific surface area is lower than ZSM5, the removal is better than ZSM5. This also confirms the ability of zero iron in reduction of nitrate through electrochemical reactions.

FTIR spectrum of ZSM5 and NZVI@ZSM5 in KBr is presented in Fig. 3. Exactly the same amount of ZSM5 and NZVI@ZSM5 was mixed with KBr powder in KBr tablet preparation. Zero-valent iron has no peaks at IR regions, and nano-zero-valent iron cannot be detected by FTIR, but ZSM5 which contains metal oxides of silicate, aluminum, and sodium has shown their corresponding M–O bands. M–O bands intensity decreases due to the quantitative relation between ZSM5 components concentration and peak intensity. However, FTIR just identifies the ZSM5. Therefore, asymmetric stretching of Si–O–Si band at about 1100 cm⁻¹ is clearly observed. Stretching vibration of Si–O appears at about 451, 793, and 900 cm⁻¹. Peaks appeared at 500–700 are also related to Al–O, and alkaline and alkaline earth oxides such as Na–O, Ca–O and Mg–O. FTIR patterns are well matched with those of ZSM5 synthesized by Khatamian and Irania (Khatamiana and Irania 2009).

Comparing NZVI and NZVI@ZSM5 reactivity

Nano-zero-valent iron is extremely reactive and needs more precautions while using in remediation studies. Preliminary experiments showed that the bare NZVI was not as stable as NZVI@ZSM5 and burned into iron oxide immediately after the exposure to the surrounding atmosphere. This mixture of Fe and magmite has reduced its nitrate remediation ability compared to NZVI@ZSM5. Observation for nitrate removal using bare NZVI is consistent with previous data obtained by Shekarriz et al. (2010). However, the stability of prepared NZVI@ZSM5 particles was high, so there was enough weighing and transfer time prior to the remediation studies.

Nitrate remediation

The synthesized nano-composite was checked for reduction of nitrate from aqueous solution. To apply that, batch experiments were performed. However, to achieve the highest possible removal ability of the present nanoparticles, the effect of different parameters such as pH, amount of NZVI@ZSM5 and contact time along with initial nitrate concentration and volume at 25°C was evaluated.



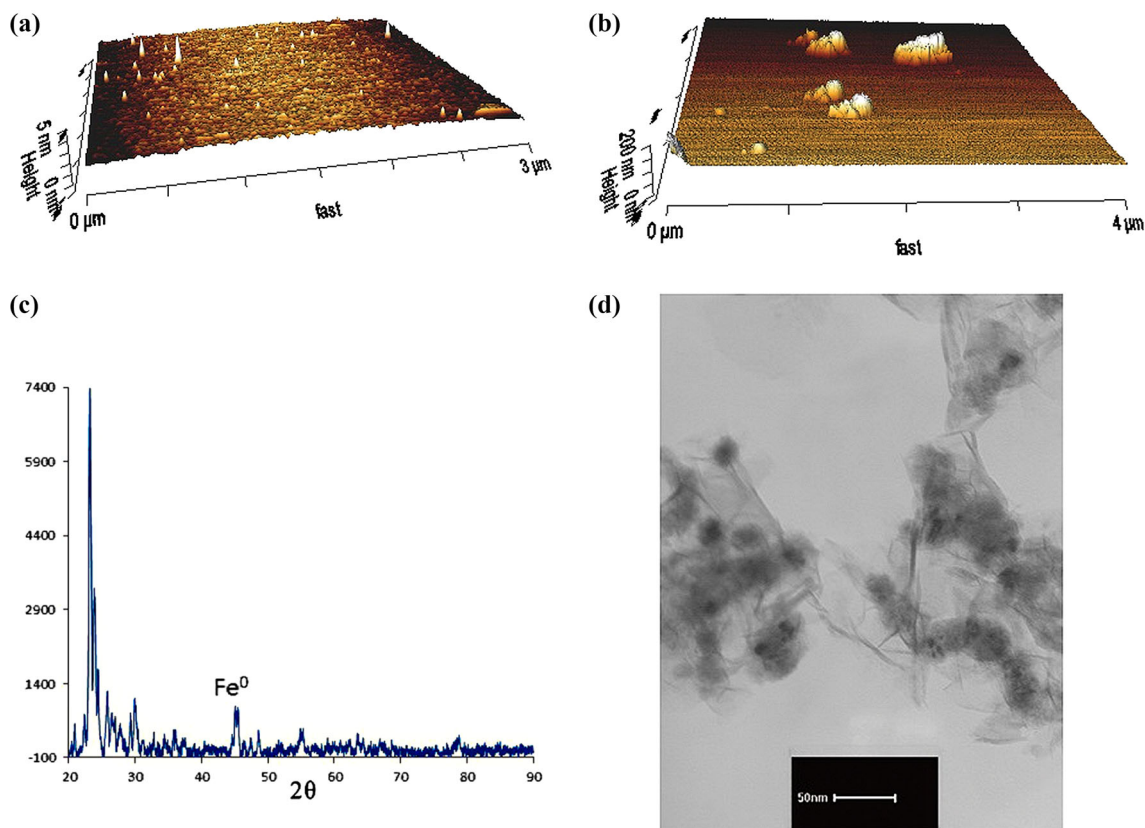


Fig. 1 AFM image of **a** NZVI@ZSM5, **b** ZSM5, **c** XRD patterns of synthesized NZVI@ZSM5 particles, and **d** TEM image of prepared NZVI@ZSM5

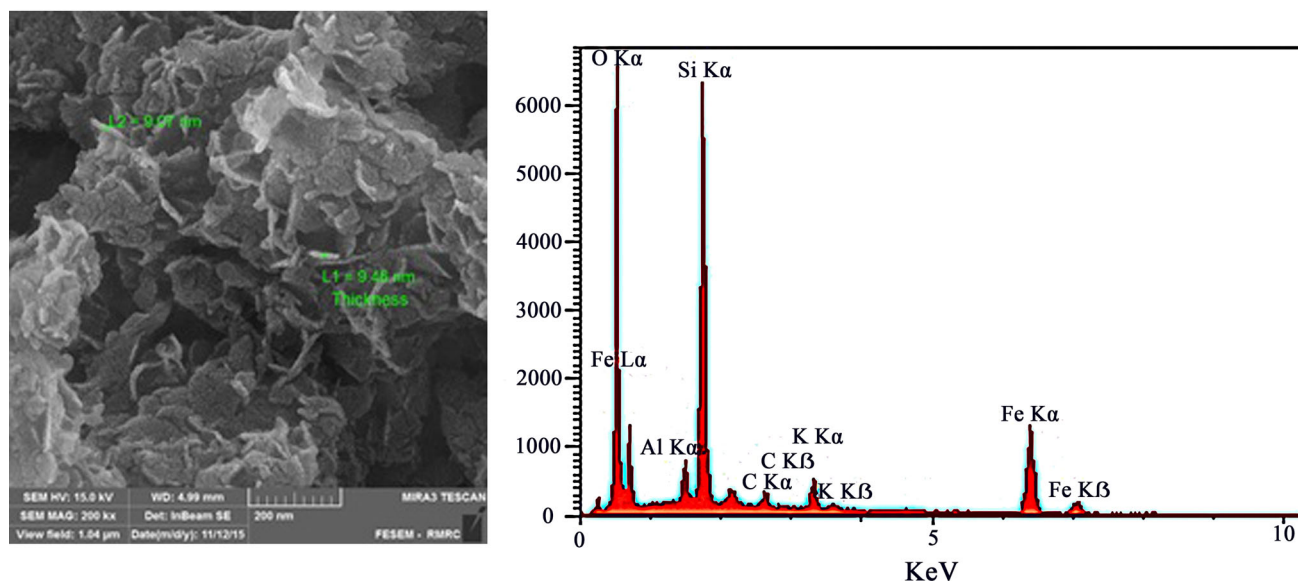


Fig. 2 FESEM image **a** and EDXS **b** of prepared NZVI@ZSM5

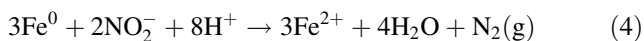
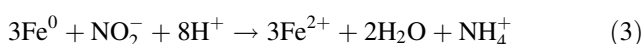
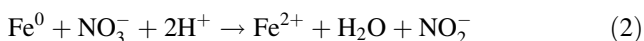
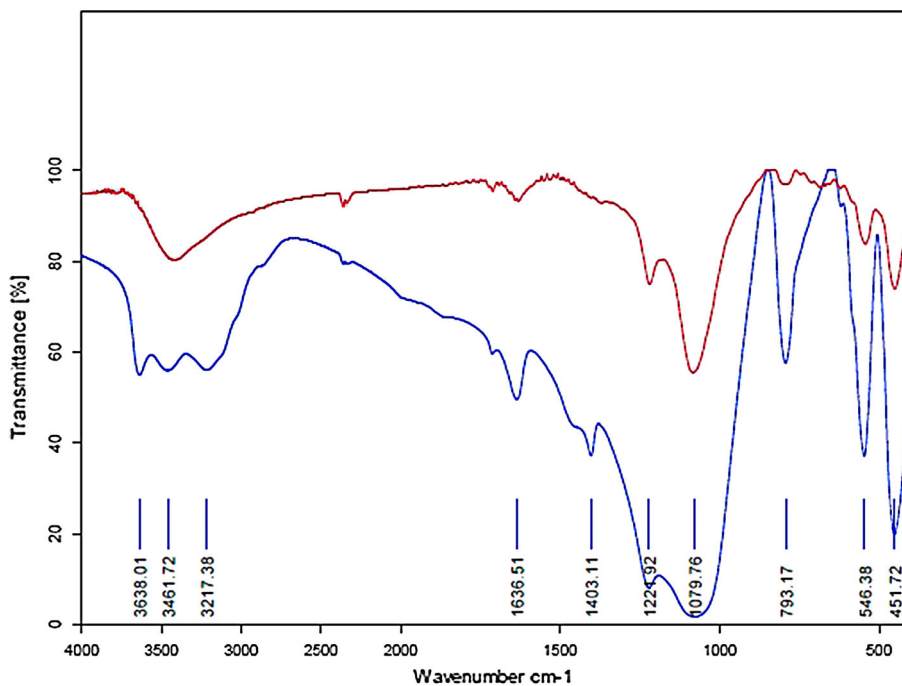
Effect of pH

Acidity has great effect on nitrate remediation in the presence of NZVI. The nature of the reaction between

nitrate and NZVI is oxidation–reduction. NZVI reduces nitrate to nitrite, ammonium, or nitrogen according to the acidity of the solution. The mechanisms for nitrate removal by NZVI are brought in Eqs. (2)–(4) (Kassaei et al. 2011)



Fig. 3 FTIR spectra of *a* ZSM5 and *b* NZVI@ZSM5



Moreover, NZVI action in nitrate removal is well established in the acidic media. First step in the nitrate remediation by NZVI is effective contact between the reagents. At low pH, the surface charge of NZVI@ZSM5 is positive (Fig. 4) and can strongly adsorb nitrate and speeds up the remediation through redox reaction, while at high pH, the surface charge reverses and repulsion forces dramatically decrease nitrate adsorption on the particle surface. This is also confirmed by the data presented graphically in Fig. 4. Hence, the optimum pH for nitrate remediation by the present particle was 2.5. Furthermore, in order to check the necessity of the high acid content of this remediation reaction, the nitrite content of the solution after nanoparticle contact was determined by Griss–Saltzman method. According to the results, no nitrite residue was detected at higher pH. The absence of ammonium was also tested by adding NaOH to the solution after nitrate removal and detecting the ammonia evolution using a litmus paper placed above the solution. Of course a precise measurement of low concentration of ammonium by methods such as capillary electrophoresis is required to decisively prove this conversion. It was previously reported that metal oxides can adsorb ammonium (Westerhoff and James 2003). ZSM5 contains mixture of different metal oxides. So it can assume that the produced ammonium during remediation was adsorbed on

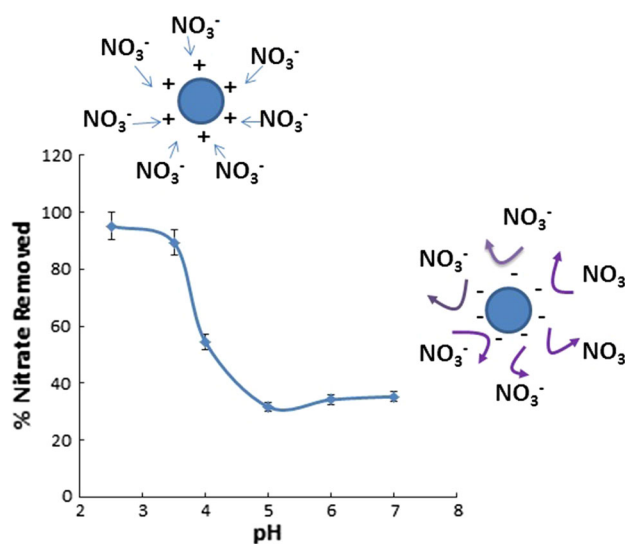


Fig. 4 Effect of pH on the nitrate remediation by NZVI@ZSM5

ZSM5 and no contaminant was present in the aqueous media after remediation. However, it was assumed that all nitrates may be converted to N_2 .

Amount of NZVI@ZSM5

As illustrated in Fig. 5, an increase in the amount of NZVI@ZSM5 particles increases nitrate elimination extensively up to 0.55 g. After that gradual increase in the nitrate removal is observed. At lower particle concentration, the iron content is not enough for the complete reaction with 50 mg mL^{-1} nitrate. At higher doses of the

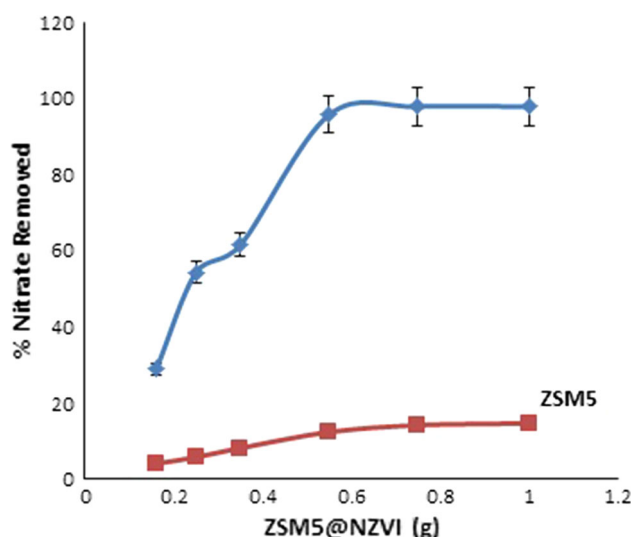


Fig. 5 Effect of the amount of NZVI@ZSM5 on nitrate remediation at pH = 2.5

particles, the maximum capacity is reached. Hence, 0.55 g was selected as optimum value since higher amount remains almost unreacted in the solution.

Contact time

The nitrate removal using zero-valent iron has shown oxidation reduction mechanism as it is depicted in Eqs. 1–3 (Suzuki et al. 2012). Therefore, the reaction has two steps. Firstly, nitrate ions should be carried to the surface of the particle, and secondly the reduction between the adsorbed nitrate and NZVI occurs. However, the contact time between the particles and nitrate solution has a great effect on the remediation. Figure 6 indicates that nitrate removal kinetic is fast and reaches a plateau after 20 min for all studied concentrations. In order to improve the robustness of the remediation, 30 min was used as optimum contact time. The removal time is considerably below the one obtained in the similar study using different sizes of zero-valent iron (Kassae et al. 2011). This may occur as a result of both protecting effect and catalytic action of ZSM5 used as the support for NZVI. Su et al. (2014) reported that bimetallic mixture of NZVI improves its remediation ability.

Initial nitrate concentration and volume

The removal ability of 0.55 g NZVI@ZSM5 at pH = 2.5 for different initial nitrate concentrations in the range of 10–100 $\mu\text{g mL}^{-1}$ was investigated. The nitrate concentrations were selected according to the wastewater nitrate permitted level. The experimental results showed that the removal efficiency reaches almost its highest value at

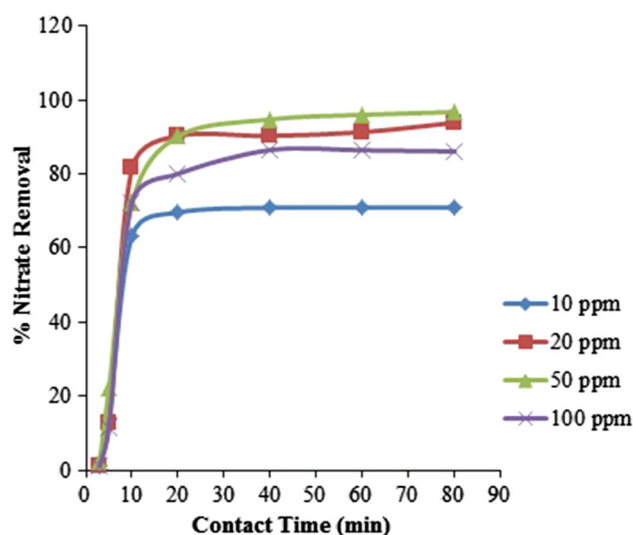
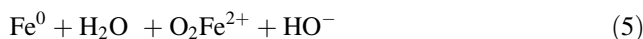


Fig. 6 Effect of contact time between NZVI@ZSM5 and nitrate solution on the removal efficiency at pH = 2.5

20 min for all tested concentrations. A slight decrease in the removal efficiency for 100 $\mu\text{g mL}^{-1}$ may be due to the limited doses of nanoparticles.

Initial nitrate solution volume is another important factor and has a considerable effect on the remediation. Increasing the volume of 50 $\mu\text{g mL}^{-1}$ nitrate solution from 50 to 100 mL causes about 20% increase in the removal ability. Further increase in volume decreases the removal. An increase in volume causes more particles dispersion in the solution, and one expects more adsorption. But further increase in the solution volume provides more dissolved oxygen available for surface deactivation of the nano-zero-valent iron. It may change the solution pH that can be described well by Eq. (5). Figure 7 graphically illustrates the results.



Adsorption isotherm

As it was mentioned before, nitrate should be adsorbed on the particle surface before reduction. In order to identify the adsorption mechanism, different adsorption isotherms listed in Table 1 were applied. Linear form of Langmuir Adsorption Isotherm that was used to calculate the corresponding isotherm equation is:

$$\frac{C_e}{q_e} = \frac{1}{q_m K_L} + \frac{C_e}{q_m} \quad (6)$$

where C_e = the equilibrium concentration of adsorbate (mg/L), q_e = the amount of metal adsorbed per gram of the adsorbent at equilibrium (mg/g), q_m = maximum monolayer coverage capacity (mg/g), and K_L = Langmuir isotherm constant (L/mg).

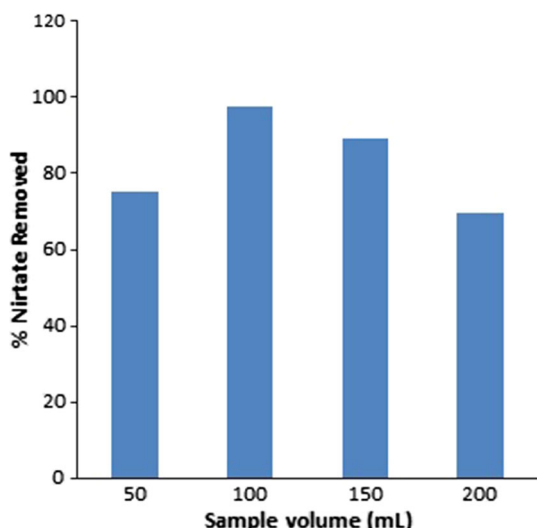


Fig. 7 Percent nitrate removed for different initial solution volume of 50 µg mL⁻¹ nitrate at optimum conditions

Table 1 Different isotherm parameters

Isotherms	Parameters	Parameters amount
Langmuir isotherm	Q_m (mg/g)	11.66
	K_a (L/mg)	0.9835
	R^2	0.9386
Freundlich isotherm	$1/n_f$	0.3599
	K_f (L/mg)	3.724
	R^2	0.5048
Temkin isotherm	B_1	1.44
	K_T (L/mg)	56.75
	R^2	0.6735
Dubinin–Radushkevich isotherm	Q_s (mg/g)	11.88
	B	3×10^7
	E (kJ/mol)	1290.99
	R^2	0.881

The essential features of the Langmuir isotherm can be expressed in terms of R_L , which is a dimensionless constant referred to as separation factor and defined as:

$$R_L = \frac{1}{(1 + K_L C_0)} \tag{7}$$

where C_0 is the initial concentration and R_L value indicates the adsorption nature. The $R_L > 1$, $R_L = 1$, $0 < R_L < 1$, and $R_L = 0$ identify unfavorable, linear, favorable, and irreversible adsorption, respectively.

The empirical equation proposed by Freundlich is

$$q_e = K_f C_e^{1/n} \tag{8}$$

where K_f = Freundlich isotherm constant (mg/g), n = adsorption intensity, C_e = the equilibrium

concentration of adsorbate (mg/L), q_e = the amount of metal adsorbed per gram of the adsorbent at equilibrium (mg/g).

Linear form of the equation has the following form:

$$\log q_e = \log K_f + \frac{1}{n} \log C_e \tag{9}$$

The constant K_f is an approximate indicator of adsorption capacity, while $1/n$ determines the adsorption strength in the adsorption process.

The Temkin model is given by the following equation

$$q_e = \frac{RT}{b_T} \text{Ln}A_T + \frac{RT}{b_T} \text{Ln}C_e \tag{10}$$

$$B = \frac{RT}{b_T} \tag{11}$$

A_T = Temkin isotherm equilibrium binding constant (L/g), b_T = Temkin isotherm constant, R = universal gas constant (8.314 J/mol K), T = temperature at 298 K, B = constant related to heat of sorption (J/mol).

Dubinin–Radushkevich isotherm (DRK) model and its linear form are described by the following equations

$$q_e = q_s e^{(-B_{DR} \varepsilon^2)} \tag{12}$$

$$\text{Ln}q_e = \text{Ln}q_s - B_{DR} \varepsilon^2 \tag{13}$$

where q_e = amount of adsorbate in the adsorbent at equilibrium (mg/g), q_s = theoretical isotherm saturation capacity (mg/g), B_{DR} = Dubinin–Radushkevich isotherm constant (mol^2/J^2). Mean free energy of adsorption (E) can be determined by $E = \frac{1}{\sqrt{2B_{DR}}}$ (Shafeeq et al. 2012). The ε can be calculated using $\varepsilon = RT \ln \left[1 + \frac{1}{C_e} \right]$

Comparison of R^2 values of the different isotherms indicates that Langmuir (0.936) is the best description of the adsorption process. The obtained R_L value was between 0 and 1 that indicates favorable adsorption.

According to the results, it may be suggested that a chemical adsorption takes place between nitrate ion and NZVI@ZSM5 species.

Kinetic study

First- and second-pseudo-orders as well as interparticle diffusion models were applied to identify the kinetic of the remediation. 100 mL of 50 ppm nitrate solution got into contact with NZVI@ZSM5 at optimum conditions. Equilibrium concentration was determined after the filtration of the solution at different time intervals. Data were fitted to the first-order (Eq. 14) and second-order (Eq. 15) kinetic equations.

Table 2 Kinetic model parameters

Model	Parameters	Parameters amount
First-order kinetic	K_1	0.0329
	q_e (calc)	2.0950
	R^2	0.3468
Second-order kinetic	$K_2 \times 10^3$	0.0401
	q_e (calc)	9.3023
	R^2	0.9998
	H	0.139
Intraparticle diffusion	K_{diff}	0.7273
	C	2.61
	R^2	0.6139
Elovich	β	0.585
	α	5.152
	R^2	0.7192

$$\ln(qe - qt) = \ln qe - k_1 t \quad (14)$$

$$\frac{t}{q_t} = \frac{1}{k_2 q_e^2} + \frac{t}{q_e} \quad (15)$$

where K_1 and K_2 are first-order and second-order kinetic rate constants, respectively, q_e is milligram nitrate adsorbed on 1 g NZVI@ZSM5 at equilibrium, q_t is milligram nitrate adsorbed on 1 g NZVI@ZSM5 at time t . The Elovich equation, originally presented in 1939, is satisfied in chemical adsorption processes.

$$q_t = \frac{1}{\beta} \ln(\alpha\beta) + \frac{1}{\beta} \ln(t) \quad (16)$$

The terms α and β in the equation are initial adsorption rate in $\text{mg g}^{-1} \text{min}^{-1}$ and Elovich constant (g mg^{-1}), consequently.

The initial rate of intraparticle diffusion is calculated by the linearization of the curve

$$q_t = K_{diff} t^{1/2} + C \quad (17)$$

Data in Table 2 indicate that the second-order model shows the best fit for the experimental data. Therefore, the first step, adsorption of nitrates on the surface of the nanoparticles, is the rate-determining step.

Table 3 Nitrate removal from wastewater of different companies located in Khuzestan province, Iran, at pH = 2, contact time = 30 min, and sample volume = 100 mL

Company location	Nitrate (mg/ml)		% Removed
	Before	After	
Gotvand	290.8187 ± 0.58	3.3859 ± 0.25	98.84
Dezful	306.3081 ± 0.46	15.1428 ± 0.49	95.06
Chamgolak	263.4484 ± 0.24	2.8216 ± 0.27	98.92
Ahvaz1	90.1998 ± 0.15	4.7027 ± 0.11	94.79
Ahvaz2	115.8760 ± 0.12	2.1632 ± 0.28	98.13

Nitrate removal for industrial wastewater

Tap, surface and river as well as wastewater of different industries contain so many cations and anions such as Fe^{3+} , Ca^{2+} , Mg^{2+} , Pb^{2+} , Cd^{2+} , Cl^- , SO_4^{2-} and CO_3^{2-} that may interfere in nitrate remediation through changes in the ionic strength or competition in the adsorption and/or reduction by the NZVI particles. Sometimes, co-ions such as cadmium can enhance the removal ability through their catalytic activity after conversion to zero-valent cadmium (Su et al. 2014). However, it could be helpful to evaluate the removal at optimized condition for nitrate contaminated industrial wastewater rather than investigation of the ionic strength by salts such as NaCl. To accomplish that, several wastewater from different industrial companies in the Khuzestan province were collected according to the sampling protocol under supervision of Ahvaz water and wastewater organization. Then, a pair of homogenized collected wastewater having certain volume (100 mL) was selected for each industrial sample. One of them received no treatment, while the other was subjected to nitrate remediation at optimized condition using NZVI@ZSM5. Finally, nitrate concentrations of both samples were determined and percent of nitrate removed was calculated. The matrix has strong effect on the remediation since incredible removal is possible even at high nitrate concentrations in the selected wastewaters. Data are presented in Table 3.

Comparing to other reported methods

Table 4 summarizes some reports on nitrate remediation using zero-valent irons. Comparing the results of commercial NZVI and surfactant-coated NZVI, we obtained faster and higher efficiency of nitrate removal while the nanoparticles are coated with surfactant. The same changes in the removal efficiency were observed while using different supports such as zeolite and pillared clay. The results of Zhang et al. (2011) are approximately the same as those obtained in the present study, but they work under anaerobic condition. NZVI@ZSM5 has shown about 97% nitrate removal at about 30 min under aerobic condition.

Table 4 Comparison of the results obtained by the present study with some recently reported ones

Method	g/l	Conc.NO ₃ mg/l	% Removed	Time (min)	References
Fe commercial	4	96	<2	85	Shekarriz et al. (2010)
NZVI (8–18 nm surfactant-coated)	4	96	96.8	30	Shekarriz et al. (2010)
Zeolite	15	100	78	120	Naej et al. (2012)
NZVI@zeolite	7.5	100	97.8	50	Naej et al. (2012)
Pillared clay	1	50	<10	120	Zhang et al. (2011)
NZVI (30–50 nm)	1	50	62.3	120	Zhang et al. (2011)
NZVI@pillared clay (under anaerobic condition)	1	50	100	120	Zhang et al. (2011)
Arc fabricated NZVI	1.33	5–30	78	720	Kassaei et al. (2011)
			92	1440	
			96	2880	
ZSM5	10	50	<15	60	Present research
NZVI@ZSM5	5.5	5–100	99	30	Present research

The present method shows higher speed and reasonable nitrate removal compared to the most reported methods.

Conclusion

To sum it up, the present study shows that ZSM5-supported NZVI particles efficiently remove nitrate in 30 min under aerobic condition. This particle can also be successfully applied in water and wastewater refinement systems under aerobic condition. In addition to NZVI stability, the catalytic action of metal oxides presented in ZSM5 may be responsible for the increase in the removal of nitrate.

Acknowledgements The financial support of Payame Noor University, Nanotechnology Research Center of Ahvaz Jundishapur University of Medical Sciences, and Research Institute of Petroleum Industry is acknowledged. We gratefully thank the warm collaboration of the Ahvaz water and wastewater agency.

References

- Ayyasamy PM, Rajakumar S, Sathishkumar M, Swaminathan K, Shanthy K, Lakshmanaperumalsamy P, Lee S (2009) Nitrate removal from synthetic medium and groundwater with aquatic macrophytes. *Desalination* 242:286–296
- Baek K, Yang J-W (2004) Cross-flow micellar-enhanced ultrafiltration for removal of nitrate and chromate: competitive binding. *J Hazard Mater* 108:119–123
- Bhardwaj D, Sharma M, Sharma P, Tomar R (2012) Synthesis and surfactant modification of clinoptilolite and montmorillonite for the removal of nitrate and preparation of slow release nitrogen fertilizer. *J Hazard Mater* 227–228:292–300
- Bhatnagar A, Kumar E, Sillanpää M (2010) Nitrate removal from water by nano-alumina: characterization and sorption studies. *Chem Eng J* 163:317–323
- Björger M, Joensen F, Holm MS, Olsbye U, Lillerud KP, Svelle S (2008) Methanol to gasoline over zeolite H-ZSM-5: improved catalyst performance by treatment with NaOH. *Appl Catal A* 345:43–50
- Busch J, Meißner T, Potthoff A, Bleyl S, Georgi A, Mackenzie K, Trabitzzsch R, Werban U, Oswald S (2015) A field investigation on transport of carbon-supported nanoscale zero-valent iron (nZVI) in groundwater. *J Contam Hydrol* 181:59–68
- Cengeloglu Y, Tor A, Ersoz M, Arslan G (2006) Removal of nitrate from aqueous solution by using red mud. *Sep Purif Technol* 51:374–378
- Chatterjee S, Woo SH (2009) The removal of nitrate from aqueous solutions by chitosan hydrogel beads. *J Hazard Mater* 164:1012–1018
- Chatterjee S, Lee DS, Lee MW, Woo SH (2009) Nitrate removal from aqueous solutions by cross-linked chitosan beads conditioned with sodium bisulfate. *J Hazard Mater* 166:508–513
- Chen Z, Wang T, Jin X, Chen Z, Megharaj M, Naidu R (2013) Multifunctional Kaolinite supported nano scale zero-valent iron used for adsorption and degradation of crystal violet in aqueous solution. *J Colloid Interface Sci* 398:59–66
- Cho D-W, Chon C-M, Kim Y, Jeon B-H, Schwartz FW, Lee E-S, Song H (2011) Adsorption of nitrate and Cr(VI) by cationic polymer-modified granular activated carbon. *Chem Eng J* 175:298–305
- Demiral H, Gündüzoğlu G (2009) Removal of nitrate from aqueous solutions by activated carbon prepared from sugar beet bagasse. *Bioresour Technol* 101:1675–1680
- Devadas A, Vasudevan S, Epron F (2011) Nitrate reduction in water: influence of the addition of a second metal on the performances of the Pd/CeO₂ catalyst. *J Hazard Mater* 185:1412–1417
- Dyer A (1988) An introduction to zeolite molecular sieves. Wiley, Australia, pp 149
- Gómez MA, Hontoria E, González-López J (2002) Effect of dissolved oxygen concentration on nitrate removal from groundwater using a denitrifying submerged filter. *J Hazard Mater* 90:267–278
- Islam M, Patel R (2011) Physicochemical characterization and adsorption behavior of Ca/Al chloride hydroxalcalite-like compound towards removal of nitrate. *J Hazard Mater* 190:659–668
- James CF (2000) The chemical reduction of nitrate in aqueous solution. *Coord Chem Rev* 199:159–179
- Karimi B, Rajaei MS, Koulivand A, Cheshmeh Soltani RD (2014) Performance evaluation of advanced Fe⁰/Fe + 2/Fe + 3/H₂O₂ process in the reduction of nitrate and organic matter from aqueous solution. *Desalin Water Treat* 52:6240–6248



- Kassae MZ, Motamedi E, Mikhak A, Rahnamaie R (2011) Nitrate removal from water using iron nanoparticles produced by arc discharge vs. reduction. *Chem Eng J* 166:490–495
- Katal R, Baei MS, Rahmati HT, Esfandian H (2011) Kinetic, isotherm and thermodynamic study of nitrate adsorption from aqueous solution using modified rice husk. *J Ind Eng Chem* 18:295–302
- Khatamiana M, Irania M (2009) Preparation and characterization of nanosized ZSM-5 zeolite using kaolin and investigation of kaolin content, crystallization time and temperature changes on the size and crystallinity of products. *J Iran Chem Soc* 6:187–194
- Kumar NS, Goel S (2010) Factors influencing arsenic and nitrate removal from drinking water in a continuous flow electrocoagulation (EC) process. *J Hazard Mater* 173:528–533
- Li J, Li Y, Meng Q (2010) Removal of nitrate by zero-valent iron and pillared bentonite. *J Hazard Mater* 174:188–193
- Liu Y, Li S, Chen Z, Megharaj M, Naidu R (2014) Influence of zero-valent iron nanoparticles on nitrate removal by *Paracoccus* sp. *Chemosphere* 108:426–432
- Ma J, Yang Q, Wang S, Wang L, Takigawa A, Peng Y (2010) Effect of free nitrous acid as inhibitors on nitrate reduction by a biological nutrient removal sludge. *J Hazard Mater* 175:518–523
- Mena-Duran CJ, Kou MRS, Lopez T, Azamar-Barrios JA, Aguilar DH, Dominguez MI, Odriozola JA, Quintana P (2007) Nitrate removal using natural clays modified by acid thermoactivation. *Appl Surf Sci* 253:5762–5766
- Naej OB, Mohseni BA, Jafari JA, Esrafil A, Rezaei KR (2012) Removal of nitrate from water using supported zero-valent nano iron on zeolite. *Iran J Health Environ* 5:343–354
- Öztürk N, Bektaş TE (2004) Nitrate removal from aqueous solution by adsorption onto various materials. *J Hazard Mater* 112:155–162
- Pan JR, Huang C, Hsieh W-P, Wu B-J (2012) Reductive catalysis of novel TiO₂/Fe₀ composite under UV irradiation for nitrate removal from aqueous solution. *Sep Purif Technol* 84:52–55
- Park H, Park Y, Yoo K, Lee S (2009) Reduction of nitrate by resin-supported nanoscale zero-valent iron. *Water Sci Techn* 59:2153–2157
- Rajakumar S, Ayyasamy PM, Shanthi K, Thavamani P, Velmurugan P, Song YC, Lakshmanaperumalsamy P (2008) Nitrate removal efficiency of bacterial consortium (*Pseudomonas* sp. KW1 and *Bacillus* sp. YW4) in synthetic nitrate-rich water. *J Hazard Mater* 157:553–563
- Shafeeq A, Muhammad A, Sarfraz W, Toqeer A, Rashid S, Rafiq MK (2012) Mercury removal techniques for industrial waste water. *Int Sci Index* 6:1180–1183
- Shekarriz M, Haghipoor S, Haji-Aliakbari F, Soleymani-Jamarani M, Kaveh-Ahangar R (2010) Optimal synthesis and nitrate and mercury removal ability of microemulsion-made iron nanoparticles. *Int J Nanoparticles* 3:123–137
- Shi L, Lin Y, Zhang X, Chen Z (2011) Synthesis, characterization and kinetics of bentonite supported nZVI for removal of Cr(VI) from aqueous solution. *Chem Eng J* 171:612–617
- Su Y, Adeleye AS, Huang Y, Sun X, Dai C, Zhou X, Zhang Y, Keller AA (2014) Simultaneous removal of cadmium and nitrate in aqueous media by nanoscale zerovalent iron (nZVI) and Au doped nZVI particles. *Water Res* 63:102–111
- Suzuki T, Moribe M, Oyama Y, Niinae M (2012) Mechanism of nitrate reduction by zero-valent iron: equilibrium and kinetics studies. *Chem Eng J* 183:271–277
- Tepuš B, Simonič M, Petrinič I (2009) Comparison between nitrate and pesticide removal from ground water using adsorbents and NF and RO membranes. *J Hazard Mater* 170:1210–1217
- Wang Y, Gao B-Y, Yue W-W, Yue Q-Y (2007a) Adsorption kinetics of nitrate from aqueous solutions onto modified wheat residue. *Colloids Surf A* 308:1–5
- Wang Y, Gao B-Y, Yue W-W, Yue Q-Y (2007b) Preparation and utilization of wheat straw anionic sorbent for the removal of nitrate from aqueous solution. *J Environ Sci* 19:1305–1310
- Wang DM, Lin HY, Shah SI, Ni CY, Huang CP (2009) Indirect electrochemical reduction of perchlorate and nitrate in dilute aqueous solutions at the Ti–water interface. *Sep Purif Technol* 67:127–134
- Wang T, Lin J, Chen Z, Megharaj M, Naidu R (2014) Green synthesized iron nanoparticles by green tea and eucalyptus leaves extracts used for removal of nitrate in aqueous solution. *J Clean Prod* 83:413–419
- Westerhoff P, James J (2003) Nitrate removal in zero-valent iron packed columns. *Water Res* 37:1818–1830
- Xu X, Gao B, Zhao Y, Chen S, Tan X, Yue Q, Lin J, Wang Y (2012) Nitrate removal from aqueous solution by *Arundo donax* L. reed based anion exchange resin. *J Hazard Mater* 203–204:86–92
- Yuh-Shan H (2005) Comment on “Nitrate removal from aqueous solution by adsorption onto various materials” by N. Öztürk, TE Bektaş. *J Hazard Mater* 118:253–254
- Zhan Y, Lin J, Zhu Z (2011) Removal of nitrate from aqueous solution using cetylpyridinium bromide (CPB) modified zeolite as adsorbent. *J Hazard Mater* 186:1972–1978
- Zhang Z, Lei Z, He X, Zhang Z, Yang Y, Sugiura N (2009) Nitrate removal by *Thiobacillus denitrificans* immobilized on poly(vinyl alcohol) carriers. *J Hazard Mater* 163:1090–1095
- Zhang Y, Li Y, Li J, Hu L, Zheng X (2011) Enhanced removal of nitrate by a novel composite: nanoscale zero valent iron supported on pillared clay. *Chem Eng J* 171:526–531
- Zhao Y, Feng C, Wang Q, Yang Y, Zhang Z, Sugiura N (2011) Nitrate removal from groundwater by cooperating heterotrophic with autotrophic denitrification in a biofilm–electrode reactor. *J Hazard Mater* 192:1033–1039

